

MERV 13 Filtration for Office Buildings During COVID-19 Pandemic

Cary A. Faulkner¹, John E. Castellini Jr.¹, Wangda Zuo^{1,2,*}, David M. Lorenzetti³, Michael D. Sohn³

¹ University of Colorado Boulder, Boulder, CO, U.S.A.

² National Renewable Energy National Laboratory, Golden, CO, U.S.A.

³ Lawrence Berkeley National Laboratory, Berkeley, CA, U.S.A.

*Corresponding email: Wangda.Zuo@colorado.edu

ABSTRACT

The COVID-19 pandemic increased the need for buildings to protect occupants from infection due to airborne pathogens. This paper investigates the use of filtration to remove viral particles in the air handling system, specifically studying trade-offs between filter quality and operational cost. While high-efficiency filters remove viral particles more effectively, they also tend to increase the pressure drop and energy use in the air handling system. Two HVAC filters are compared: (1) moderately rated MERV 10 filter and (2) more efficient MERV 13 filter. These filters are evaluated for a five-zone medium office building in a cold and dry climate, modeled using the Modelica Buildings library. New models for the HVAC filters and virus behavior are developed to support this study. The results show MERV 13 filtration reduces the average virus concentration by about 10% compared to MERV 10 filtration, but increases the annual energy consumption by about 3%.

KEYWORDS: COVID-19, Indoor Air Quality, HVAC Filtration, Modelica.

1 INTRODUCTION

Improving indoor air quality in buildings is important to reduce the risk of infection from airborne transmission during the COVID-19 pandemic. It is well known that the risk of COVID-19 infection is significant indoors. For example, one recent study (Qian et al., 2021) identified 318 outbreaks of three or more COVID-19 cases in China and found all occurred in indoor environments. Consequently, organizations like ASHRAE issued guidelines (ASHRAE, 2021) to improve indoor air quality in buildings to reduce the risk of infection. These guidelines included recommendations for operating the heating, ventilation, and air-conditioning (HVAC) system, such as achieving at least Minimum Efficiency Reporting Value (MERV) 13 level filtration for recirculating air. More efficient filters are beneficial to removing recirculating viral particles in the air handling system, but have potential negative impacts as well. Particularly, more efficient filters may be more expensive or increase the pressure drop through the air handling system with a higher fan energy consumption (Zaatari et al., 2014). Some HVAC systems may not even be sized to overcome the increased pressure drop of high efficiency filters. In this paper, we discuss the research required to quantify the trade-offs when increasing filter efficiency.

Previous literature tried to study trade-offs of HVAC filter efficiency. Azimi and Stephens (2013) compared the trade-offs of risk reduction of influenza virus and annual cost for different HVAC filters.

They found that increasing filtration efficiency is beneficial to reducing risk of infection, but reaches a level of diminishing returns for risk reduction with more significant increases in annual cost for the most efficient HVAC filters. Pease et al. (2021) investigated the effect of filtration efficiency on indoor virus concentration and probability of infection for COVID-19 virus. They also found that increasing filtration reduces risk of infection, but the risk reduction becomes relatively smaller beyond MERV 8 level filtration.

Although notable progress has been made in the literature to quantify the impacts of increased filtration efficiency, further scientific advancement can be achieved. Some of the above studies may have benefitted from the use of detailed modeling to fully account for the dynamics of the HVAC system. For example, the supply flow rates and outdoor air fractions are often assumed to be constant for a given scenario. Some also often assume steady-state virus concentrations when evaluating risk of infection. However, these values are dynamic in practice and affect the predicted risk of infection and operational cost.

This paper aims to address these considerations through detailed dynamic modeling of an HVAC system. We develop a dynamic system model based on the Modelica *Buildings* library (Wetter et al., 2014) to compare moderate MERV 10 level filtration and more efficient MERV 13 level filtration. Detailed HVAC system modeling with the Modelica language has been used to perform dynamic analyses for various applications, such as data center cooling energy efficiency (Fu et al., 2019) and chiller plant control performance (Fan et al., 2021). Additionally, new models for HVAC filters and indoor virus behavior are developed to support this study.

In Section 2 we describe the development and implementation of new models for HVAC filtration and indoor virus behavior into an existing HVAC system model for a medium office building located in a cold and dry climate. The results for indoor virus concentration and energy consumption are then summarized in Section 3. Finally, conclusions are drawn in Section 4.

2 MODEL IMPLEMENTATION

We developed an HVAC system model for a medium office building that incorporates new models to support this study. First, we describe the prototype medium office building. We then describe the new models for HVAC filtration and indoor virus behavior.

2.1 Description of Building System

The building model is based on the DOE commercial reference medium office building (Field et al., 2010; DOE), with a focus on expressing the bottom floor. This floor contains five zones as shown in Figure 1, which are assumed to be well-mixed in the model. The Core zone has a volume of 2,698 m³, the North and South zones have volumes of 569 m³, and the East and West zones have volumes of 360 m³. The HVAC system consists of a central air handling unit with heating and cooling coils that serve this floor. Each zone has variable-air-volume (VAV) terminal boxes with reheat coils, as well. The HVAC system is sized for the studied climate of Denver, Colorado, USA, which is a cold and dry climate. Cooling is provided using a chilled water system and heating is provided via a hot water system. The system is controlled based on the VAV 2A2-21232 control sequence from the Sequences of Operation for Common HVAC Systems as described in (Wetter et al., 2018).

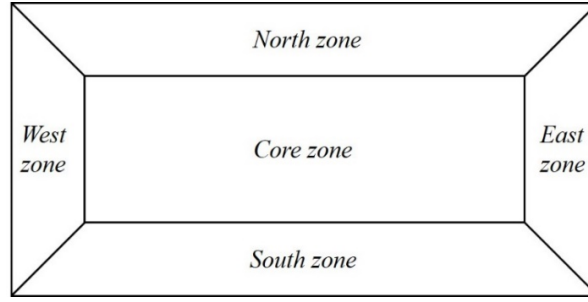


Figure 1. Floor layout of medium office building.

2.2 HVAC Filter Model

An HVAC filter model was developed to support this study. This model incorporates two key features: 1) the filtration of viral particles based on a defined efficiency value and 2) the added system pressure drop due to the filter. First, the removal of viral particles from the airflow through the filter is described as:

$$c_{out} = (1 - \eta_{filter})c_{in}, \quad (1)$$

where c_{out} is the virus concentration in the airflow leaving the filter, η_{filter} is the defined filter efficiency, and c_{in} is the virus concentration in the airflow entering the filter.

Next, the static pressure drop across the filter is calculated as:

$$\Delta p_{filter} = k_{filter} \dot{m}_{filter}^2, \quad (2)$$

where Δp_{filter} is the static pressure drop caused by the filter, \dot{m}_{filter} is the mass flow rate of airflow through the filter, and the constant k_{filter} is determined as:

$$k_{filter} = \frac{\Delta p_{nom}}{\dot{m}_{nom}^2}, \quad (3)$$

where Δp_{nom} is the nominal pressure drop for the nominal mass flow rate, \dot{m}_{nom} . As the inputs to the filter model, these values depend on the filter rating and are shown in Table 1. The filter efficiency values come from ASHRAE Standard 52 (ASHRAE, 2017) assuming viral particle diameters in the range of 1-3 μm . The values of the nominal pressure drop come from data for MERV 10 (Dwyer, a) and MERV 13 (Dwyer, b) filters. The nominal pressure drop settings are chosen based on the average initial resistance and final resistance for the nominal flow rate. A summary of the filter simulation settings is shown in Table 1.

Table 1. HVAC filter model values.

Filter	Nominal Pressure Drop (Pa)	Efficiency
MERV 10	143	50%
MERV 13	162	85%

2.3 Virus Transport Modeling

In addition, we develop new models to represent virus behavior indoors. First, we model a single “sick” person in each zone working from 9:00 AM to 5:00 PM, Monday through Friday throughout the year. These sick people generate viral particles based on a constant quanta generation rate of 100 *quanta/hr*, where a quantum is the dose of viral droplet nuclei that is expected to cause infection in 63% of susceptible people (Buonanno, 2020). The viral particles were generated in the well-mixed zones when the sick people were present.

Viral decay due to death of airborne virus was also modeled in this study. The viral decay is described as:

$$\dot{c}_{decay,zone} = k_{decay}c_{zone}, \quad (4)$$

where $\dot{c}_{decay,zone}$ is the rate of viral decay in the zone, k_{decay} is the constant rate of viral decay, and c_{zone} is the virus concentration in the zone. This equation has been used to model viral decay in well-mixed zones in the literature (Pease, 2021).

Finally, risk of infection based on the virus concentration is calculated using the Wells-Riley approach (Riley et al., 1978) as:

$$R(t) = 1 - \exp(-IR \int_{t_0}^t c(t)dt), \quad (5)$$

where $R(t)$ is the risk of infection in terms of percentage, IR is the volumetric inhalation rate of air for an occupant, and $\int_{t_0}^t c(t)dt$ is the integral of virus concentration in the room since time t_0 . The predicted number of infections in a zone can be calculated based on the risk as:

$$R_0(t) = SR(t), \quad (6)$$

where $R_0(t)$ is the predicted number of infections over time and S is the number of susceptible occupants in the zone.

3 RESULTS

The heat maps in Figure 2 show the magnitude of normalized concentration during different times of the day throughout the entire year. The normalized concentration, c_0 , is the annual average concentration for MERV 10 level filtration and is used throughout this study. The heat maps show MERV 13 level filtration reduces the magnitude of virus concentration compared to MERV 10 level filtration, as seen by the overall darker magnitudes of concentration for the MERV 10 heat map. Both heat maps follow similar trends, where the concentration increases quickly at 9:00 AM when the sick people arrive, reaches its peak during the day, then falls when the sick people leave and the virus decays and is flushed out of the building. Additionally, a higher concentration can be seen during the middle of the year, especially for MERV 10 level filtration. This is because during the summer the system tends to supply the minimum outdoor air to save on cooling energy. Since these filters do not remove 100% of viral particles, the amount of fresh outdoor air supplied also affects the virus concentration, and more so for the less efficient MERV 10 filter. Overall, MERV 13 level filtration reduces the average virus concentration throughout the year by about 10% compared to MERV 10 level filtration.

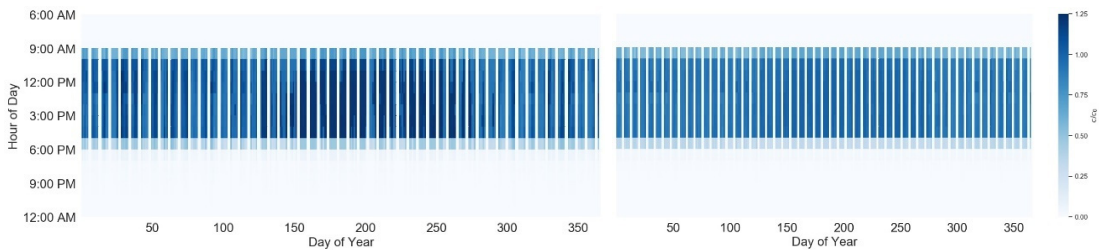


Figure 2. Heat maps showing normalized virus concentration throughout the year for MERV 10 (left) and MERV 13 (right) filtration.

Next, sample concentration results for a hot summer day in the North zone are shown. This day was chosen to show the results when the ventilation system supplies the minimum outdoor airflow, and thus relies more on the filter to remove viral particles from the building air. Figure 3 shows the results for normalized concentration and predicted number of infections for this day. The virus concentration results show MERV 13 level filtration reduces the peak concentration by about 17% compared to MERV 10 level

filtration for this day. Additionally, MERV 13 level filtration reduces the predicted number of infections on this day by about 0.31 compared to MERV 10 level filtration. This means that at least one infection is predicted in the zone for both filtration strategies, but the probability of a second infection is reduced by about 30% using MERV 13 level filtration.

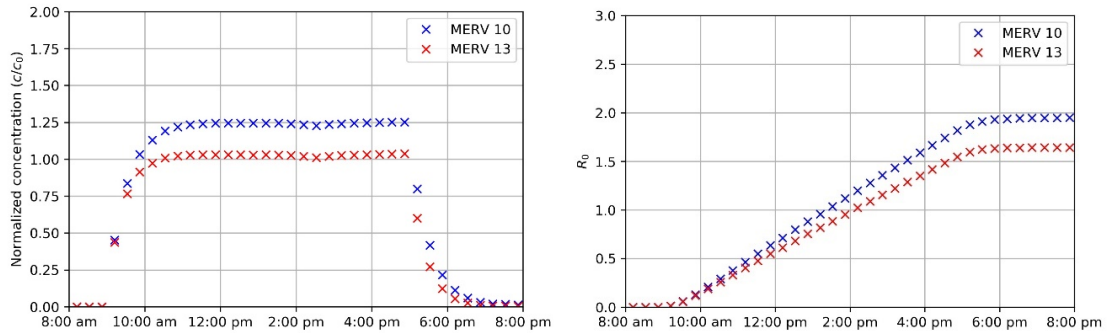


Figure 3. Normalized concentration (left) and predicted number of infections (right) for the two filters during a hot summer day.

Next, the annual energy consumption results are shown in Table 2. For this system, the fan energy is dominant, followed by the heating energy, then cooling energy. The resistance of the filters is significant to the fan energy consumption and the increased resistance of the MERV 13 filter shows about a 12% increase in fan energy usage. Interestingly, the system with the MERV 13 filter uses more cooling energy and less heating energy. This is due to the fan which dissipates heat from the motor. As the fan works harder, the amount of dissipated heat increases, which is why the MERV 13 case sees a reduction in heating energy but an increase in cooling energy. The total energy consumption increased by about 3% using MERV 13 level filtration compared to MERV 10.

Table 2. Annual Energy Consumption.

Filter	Fan Energy (MWhr)	Cooling Energy (MWhr)	Heating Energy (MWhr)	Total Energy (MWhr)
MERV 10	32.8	13.2	26.3	72.3
MERV 13	36.7	13.5	24.3	74.5

4 CONCLUSION

Use of MERV 10 and MERV 13 level filtrations during the COVID-19 pandemic were investigated for a medium office building in a cold and dry climate. The results showed MERV 13 level filtration provided better indoor air quality compared to MERV 10 level filtration and could reduce the predicted number of infections. However, use of MERV 13 level filtration increased the annual energy consumption by about 3% due to the increase in fan energy caused by the higher resistance of the MERV 13 filter. The provided models can be used to evaluate the trade-offs of strategies to improve indoor air quality during the COVID-19 pandemic, including different levels of filtration or ventilation. Furthermore, these models can be used to analyze strategies to improve indoor air quality for other virus scenarios.

5 ACKNOWLEDGEMENTS

This research was supported in part by the U.S. Defense Threat Reduction Agency and performed under U.S. Department of Energy Contract No. DE-AC02-05CH11231. This work emerged from the IBPSA Project 1, an international project conducted under the umbrella of the International Building

Performance Simulation Association (IBPSA). Project 1 will develop and demonstrate a BIM/GIS and Modelica Framework for building and community energy system design and operation.

REFERENCES

- Azimi, P., & Stephens, B. (2013). HVAC filtration for controlling infectious airborne disease transmission in indoor environments: predicting risk reductions and operational costs. *Building and environment*, 70, 150-160.
- Buonanno, G., Stabile, L., & Morawska, L. (2020). Estimation of airborne viral emission: Quanta emission rate of SARS-CoV-2 for infection risk assessment. *Environment international*, 141, 105794.
- Fan, C., Hinkelman, K., Fu, Y., Zuo, W., Huang, S., Shi, C., Mamaghani, N., Faulkner, C., & Zhou, X. (2021). Open-source Modelica models for the control performance simulation of chiller plants with water-side economizer. *Applied Energy*, 299, 117337.
- Field, K., Deru, M., & Studer, D. (2010). Using DOE commercial reference buildings for simulation studies.
- Fu, Y., Zuo, W., Wetter, M., VanGilder, J. W., Han, X., & Plamondon, D. (2019). Equation-based object-oriented modeling and simulation for data center cooling: A case study. *Energy and Buildings*, 186, 108-125.
- Pease, L. F., Wang, N., Salsbury, T. I., Underhill, R. M., Flaherty, J. E., Vlachokostas, A., Kulkarni, G., & James, D. P. (2021). Investigation of potential aerosol transmission and infectivity of SARS-CoV-2 through central ventilation systems. *Building and Environment*, 197, 107633.
- Qian, H., Miao, T., Liu, L., Zheng, X., Luo, D., & Li, Y. (2021). Indoor transmission of SARS-CoV-2. *Indoor Air*, 31(3), 639-645.
- Riley, E. C., Murphy, G., & Riley, R. L. (1978). Airborne spread of measles in a suburban elementary school. *American journal of epidemiology*, 107(5), 421-432.
- Wetter, M., Zuo, W., Nouidui, T. S., & Pang, X. (2014). Modelica buildings library. *Journal of Building Performance Simulation*, 7(4), 253-270.
- Wetter, M., Hu, J., Grahovac, M., Eubanks, B., & Haves, P. (2018, September). OpenBuildingControl: Modeling feedback control as a step towards formal design, specification, deployment and verification of building control sequences. In *Building Performance Modeling Conference and SimBuild*.
- Zaatari, M., Novoselac, A., & Siegel, J. (2014). The relationship between filter pressure drop, indoor air quality, and energy consumption in rooftop HVAC units. *Building and Environment*, 73, 151-161.
- ASHRAE. (2017). Method of Testing General Ventilation Air-Cleaning Devices for Removal Efficiency by Particle Size. Retrieved from https://www.ashrae.org/File%20Library/Technical%20Resources/COVID-19/52_2_2017_COVID-19_20200401.pdf.
- ASHRAE. (2021). Core Recommendations for Reducing Airborne Infectious Aerosol Exposure. Retrieved from <https://www.ashrae.org/file%20library/technical%20resources/covid-19/core-recommendations-for-reducing-airborne-infectious-aerosol-exposure.pdf>.
- DOE. Commercial Reference Buildings. Retrieved from <https://www.energy.gov/eere/buildings/commercial-reference-buildings>.
- Dwyer (a). MERV 10 Pleated Filters. Retrieved from https://www.dwyer-inst.com/PDF_files/Priced/DF10_cat.pdf
- Dwyer (b). MERV 13 Pleated Filters. Retrieved from https://www.dwyer-inst.com/PDF_files/Priced/DF13_cat.pdf.